

This is the postprint version of the following article: Lucío MI, Opri R, Pinto M, et al. Targeted killing of prostate cancer cells using antibody–drug conjugated carbon nanohorns. *Journal of Materials Chemistry B*. 2017;5(44):8821-8832. doi: [10.1039/c7tb02464a](https://doi.org/10.1039/c7tb02464a).

This article may be used for non-commercial purposes in accordance with RSC Terms and Conditions for Self-Archiving.

Targeted Killing of Prostate Cancer Cells using Antibody-Drug conjugated Carbon Nanohorns

María Isabel Lucío,^{a,b,c} Roberta Opri,^d Marcella Pinto,^d Alessia Scarsi,^e Jose L. G. Fierro,^f Moreno Meneghetti,^{e,*} Giulio Fracasso,^{d,*} Maurizio Prato,^{c,g,h} Ester Vázquez,^{a,b} María Antonia Herrero,^{a,b,*}

Received 00th January 20xx,
Accepted 00th January 20xx

DOI: 10.1039/x0xx00000x

www.rsc.org/

The ability of carbon nanohorns (CNHs) to cross biological barriers makes them potential carriers for delivery purposes. In this work, we report the design of a new selective antibody-drug nanosystem based on CNHs for the treatment of prostate cancer (PCa). In particular, cisplatin in a prodrug form and the monoclonal antibody (Ab) D2B, selective for PSMA⁺ cancer cells, have been attached to CNHs due to the current application of this antigen in PCa therapy. The hybrids Ab-CNHS, cisplatin-CNHS and functionalised-CNHS have been also synthesized to be used as control systems. The efficacy and specificity of the D2B-cisplatin-CNHS conjugate to selectively target and kill PSMA⁺ prostate cancer cells have been demonstrated in comparison with the other derivatives. The developed strategy to functionalise CNHs is fascinating because it can allow a fine tuning of both drug and Ab molecules attached to the nanostructure in order to modulate the activity of the nanosystem. Finally, the herein described methodology can be used for the incorporation of almost any drugs or Abs in the platforms in order to create new targeted drugs for the treatment of different diseases.

Introduction

Carbon nanohorns (CNHs) are in the shape of a single tube formed by a rolled graphene sheet with a closed horn-shaped tip. The tube has a diameter between 2 and 5 nm, a length of about 30–50 nm and normally self-assembles in spherical dahlia-like aggregates. These carbon nanostructures are emerging among others in nanomedicine due to their ideal homogenous size (\approx 80 nm), which is useful for the cellular uptake,¹ and their synthesis in absence of metal catalysts which could lead to undesired toxicity. In fact, CNHs have already been used as carriers for drug,^{2,3} as well as genetic material,^{4,5} demonstrating that they are suitable platforms for delivery purposes. However, up to now the main obstacle for the application of these nanomaterials is their lack of specificity.

Abs recognizing some tumour associated antigens (TAAs) are currently applied “naked”, conjugated to radiochemicals or to

chemotherapeutic drugs in the clinics.⁶ They have been also used to improve the selectivity of carbon nanomaterials due to their easy conjugation to the nanostructures, the high affinity and the stability,^{7–9} showing promising results in tumour diagnosis and therapy.¹⁰ Prostate cancer (PCa) is the most common cancer in man in industrialized countries and it can be often treated successfully when diagnosed in the early stages; local and regional stages show a 5-year relative survival rate nearly 100%.¹¹ Unfortunately patients where cancers have spread to distant lymph nodes, bones, or other organs show a drastic decreasing of 5-year relative survival rate (i.e. survival rate of 28%), although some surgical, chemotherapeutic or radiotherapeutic treatments (i.e. alone or in combination) are performed. Therefore new therapeutical approaches are needed and, among these, the targeted approaches based on the recognition of the cell associated tumour antigens are promising.¹²

Glutamate carboxypeptidase II (GCPII) is an enzyme expressed on the membrane of normal human prostate cells and at very low level on duodenal epithelial (brush border) cells and proximal tubule cells in the kidney.^{13–15} This enzyme, also called prostate-specific membrane antigen (PSMA), is overexpressed in PCa tissues.¹⁶ PSMA is endowed with some fascinating characteristics: i) an elevated level in metastatic and hormone refractory carcinomas; ii) an influence on the survival and proliferation of prostate tumour cells^{17,18} and iii) a peculiar expression on the neovasculature associated with other tumours.¹⁴ Therefore numerous efforts have been made in order to engineer specific antibodies against this antigen (Ag).^{19–21} Among these new Abs the clone called D2B, which recognizes an extracellular domains of PSMA, shows very high affinity and a good “in vitro” and “in vivo” specificity as reported

^a Departamento de Química Orgánica, Inorgánica y Bioquímica, Facultad de Ciencias y Tecnologías Químicas, Universidad de Castilla-La Mancha, Campus Universitario, 13071 Ciudad Real, Spain. E-mail: MariaAntonia.Herrero@uclm.es

^b IRICA Universidad de Castilla-La Mancha. Campus Universitario, 13071 Ciudad Real, Spain.

^c Department of Chemical and Pharmaceutical Sciences, University of Trieste, 34127 Trieste, Italy.

^d Department of Medicine, University of Verona, Policlinico GB Rossi, Piazzale L. A. Scuro 10, 37134 Verona Italy. Email: giulio.fracasso@univr.it

^e Department of Chemical Sciences, University of Padova, Via Marzolo, 1, II-35131, Padova, Italy. Email: moreno.meneghetti@unipd.it

^f Instituto de Catálisis y Petroleoquímica, CSIC, Cantoblanco, 28049, Madrid, Spain.

^g CIC BiomaGUNE, Parque Tecnológico de San Sebastián, Paseo Miramón, 182, 20009 San Sebastián (Guipúzcoa), Spain.

^h Basque Foundation for Science, Ikerbasque, Bilbao 48013, Spain

† Electronic Supplementary Information (ESI) available: See DOI: 10.1039/x0xx00000x

in many papers.^{22–24} Indeed, we have recently used the D2B antibody to build a sensor for the protein PSMA, as a prostate cancer biomarker, with very low limit of detection and quantification even in complex matrices.²⁵ The disadvantages of applying “naked” Abs in cancer passive immunotherapy are related to the down regulation of the target Ag in some tumour populations after the first set of treatments and/or the little efficacy of the immunological mechanisms activated after the Ab-Ag recognition. These drawbacks have addressed the researches to explore the potentiality of the Abs as targeting moiety for drugs. Ab-drug conjugates represent an innovative therapeutic system that combines the leading properties of Abs with the cell killing activity of powerful cytotoxic drugs, reducing systemic toxicity and increasing the therapeutic benefit for patients.^{26–30} However, they would suffer the same limitations of the “naked” antibodies.³¹ In addition, Ab-drug conjugates are not suitable for the incorporation of high loads of drug as this could imply a decrease of the Ab affinity to the target antigen. In this scenario CNHs could play an important role as cargo systems for the drug due to: i) their easily multi-modifiable surface; ii) their high cargo capacity; iii) their accumulation in inflamed tissues also due to enhanced permeability and retention (EPR) effect. The design of selective drug nanocarriers has been already broached using non-covalent methodologies and showing targeted killing activity *in vitro* and *in vivo*.^{32,33} Indeed nanotubes^{34–41} and nanohorns^{2,42–45} have been applied to improve the uptake and selectivity of cisplatin, a well-known chemotherapeutic drug currently applied in the treatment of many solid tumours.⁴⁶ These delivery approaches highlight that the covalent functionalization is an intriguing alternative to control the uptake and release of the drug. Furthermore, considering that the activity of platinum (II) drugs can get lost before arriving to cells,⁴⁷ the use of more inert platinum (IV) compounds as prodrugs are springing up to avoid the deactivation.⁴⁸ In fact, carbon nanotubes has been previously studied as carrier for Pt (IV) prodrugs, which releases Pt (II) inside the cells by the reduction caused by low-pH of tumour microenvironment and intracellular organelles as endosomes.⁴⁹ In this way, we are taking into account the feasible orthogonal multi-functionalization of CNHs previously optimized in our lab⁵⁰ and their excellent properties to act as delivery systems in order to get selective drugs. Concretely, the objective of this work was the design of a new CNH based platform which carries an antineoplastic agent (cisplatin) together with a targeting moiety, the anti-PSMA D2B Ab, for the specific intoxication of PCa cells. Other derivatives were synthesized together with our hybrid Ab-CNH-drug in order to have a comparative analysis of their behaviour in cells (i.e. functionalised CNHs without Ab and drug and CNHs functionalised only with drug or with Ab). All the complexes were fully characterized using various techniques, such as UV-Vis-NIR spectroscopy, Raman spectrometry, transmission electron microscopy (TEM) and thermogravimetric analysis (TGA), and finally, they were assayed to investigate the selectivity and activity towards cancer cells. The main text of the article should appear here with headings as appropriate.

Results and Discussion

Synthesis of the α -amino acid, the aniline, the prodrug and modification of the D2B antibody

The α -amino acid 4 and the aniline 6 (scheme 1 and 2) were used to get the double functionalization of CNHs via a 1,3-dipolar cycloaddition and a radical addition. They were chosen in order to have two different protected groups that can be selectively deprotected and long chains that could afford solubility. Their synthesis was carried out according to the literature.^{50–53}

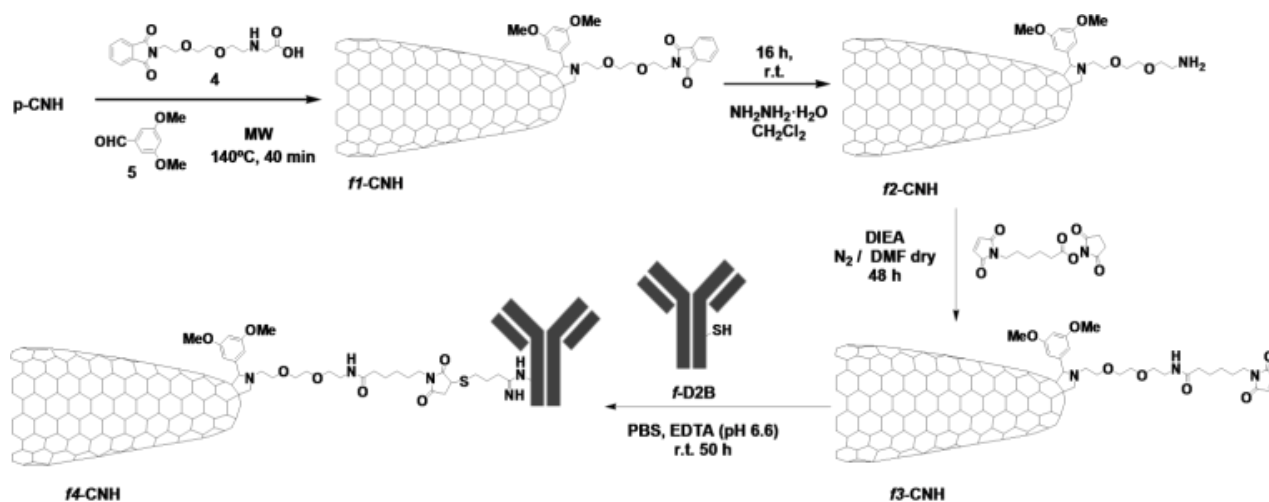
The Pt (IV) prodrug 3 was synthesized following the previously described procedure (Fig. S1, ESI†).⁵⁴ Cisplatin was firstly oxidized in ethanolic hydrogen peroxide under N_2 affording the intermediate 2 in 98% yield. In the next reaction, the hydroxide of the complex reacted with succinic anhydride under N_2 producing the cisplatin derivative 3 in 35% yield, capable of being attached to an amine-functionalised CNH through the carboxyl group. This prodrug 3 is able to release the toxic molecule cisplatin upon intracellular reduction caused by low pH environment.⁵⁴

The chosen methodology to attach the Abs to the CNHs is an addition of thiol groups on the previously inserted maleimide chains. Therefore, a modification of D2B Ab was performed applying 2-iminothiolane (2-IT, Traut's reagent) in order to increment the number of accessible thiol groups.⁵⁵ The amount of thiols were determined by Ellman's assay⁵⁶ showing an average of one thiol group per antibody.

Synthesis and characterisation of carbon nanohorns derivatives

Ab-CNTs derivatives have demonstrated to bind specific target Ags on cancer cells in a selective way. The choice of creating a covalent bond can provide a more chemically stable conjugate and prevent the premature release of the Abs due to their exchange with other proteins present in serum, onto nanotube surface.^{25,57} Therefore, we used this approximation to build similar hybrids with CNHs.

As a first approach, the synthesis of the Ab-functionalised CNHs was addressed (scheme 1). Firstly, we carried out a 1,3-dipolar cycloaddition on the pristine carbon nanohorns (p-CNH) using the phthalimide-protected amino acid 4 and the aldehyde 5 under microwave irradiation.⁵⁰ Then, a basic medium (hydrazine in dichloromethane) was applied to deprotect the necessary amine groups for the next step. The thermogravimetric analysis of the sample f2-CNH showed a weight loss of 15% at 600 °C under N_2 (Fig. S2, ESI†; table 1,) corresponding to 484 μmol of functional group per gram of carbon nanohorns and it was consistent with the positive Kaiser test (121 μmol of amino groups/g CNH), which determines the free amine groups in organic compounds.⁵⁸



Scheme 1 Synthesis of functionalised carbon nanohorns f4-CNH.

The low value of the Kaiser tests in comparison with the TGA data is attributed to the low solubility of the carbon nanostructures which prevents the titration of all the amino compounds by UV-Vis-NIR spectroscopy. The posterior reaction of f2-CNH with 6-maleimido-hexanoic acid N-hydroxysuccinimide (NHS) ester yielded the f3-CNH intermediate (18% weight loss, N₂, 600 °C, Fig. S2, ESI[†], table 1), corresponding to 336 μmol of functional group per gram of CNHs and negative Kaiser Test). This hybrid incorporates a maleimide group for the next binding to of sulfhydryl groups of the Ab.

Table 1 Functionalization data based on TGA results and qualitative Kaiser Test.

Sample	TGA, N ₂ , Weight loss at 600°C	μmol F.G./g CNHs (TGA)	μmol amino group/g CNHs Kaiser Test
f2-CNH	15%	484	121
f3-CNH	18%	336	≈ 0
f4-CNH	34%	1.06 [a]	n/a
f5-CNH	23%	308[b]	≈ 0
f6-CNH	20%	319[b]	100
f7-CNH	17%	257[c]	139
f8-CNH	23%	194[d]	≈ 0
f9-CNH	22%	110c	118

[a] Number of antibodies. [b] Chains of functional groups introduced by the radical addition of anilines. [c] chains of functional groups introduced by 1,3-dipolar cycloaddition and [d] chains of introduced maleimide groups.

In the last stage, the thiolated Ab (f-D2B) was attached to the maleimido groups by reaction in PBS-EDTA (4 μM) at pH = 6.6, during 60 h. The reaction was carried out at this pH to avoid hydrolysis of the maleimido group⁵⁷ and regeneration of 2-IT.⁵⁹

The success of the addition was demonstrated by the absence of free thiol groups in the crude of reaction by Ellman's test. After cleaning with PBS-EDTA (4 μM), f4-CNH was analysed by thermogravimetric analysis, observing a weight loss of 34% at 600 °C under N₂ (Fig. S2, ESI[†]; table1), corresponding to 1.06 μmol of Ab per gram of CNHs.

Once the synthesis of the Ab-CNH f4-CNH was achieved, the synthesis of the hybrid Ab-CNH-drug f11-CNH was carried out. The derivative without Ab and drug (f7-CNH) and the one with drug but without Ab (f10-CNH) were synthesized throughout the same synthetic route (control samples). The preparation of all hybrids is summarized in scheme 2.

In a first step, starting from the derivative functionalised by 1,3-dipolar cycloaddition f1-CNH, a new chain with an orthogonal protective group 6 was introduced in CNHs following the same procedure previously described by our group.⁵⁰ The yielded hybrid f5-CNH possesses two different protected focal points which allow the incorporation of different molecules. Based on TGA analysis (Fig. S4, ESI[†]) we introduced 308 μmol of Boc-protected functional group per gram of CNHs in the arene radical addition on the nanohorns previously functionalised with phthalimide-protected functional group. This implies the introduction of 1 Boc-protected functional group every approximately 190 carbon atoms, value that agree with the previously reported ones.⁵⁰ These data were calculated from the difference between the total weight loss and the weight loss after the 1,3-dipolar cycloaddition in the TGA.

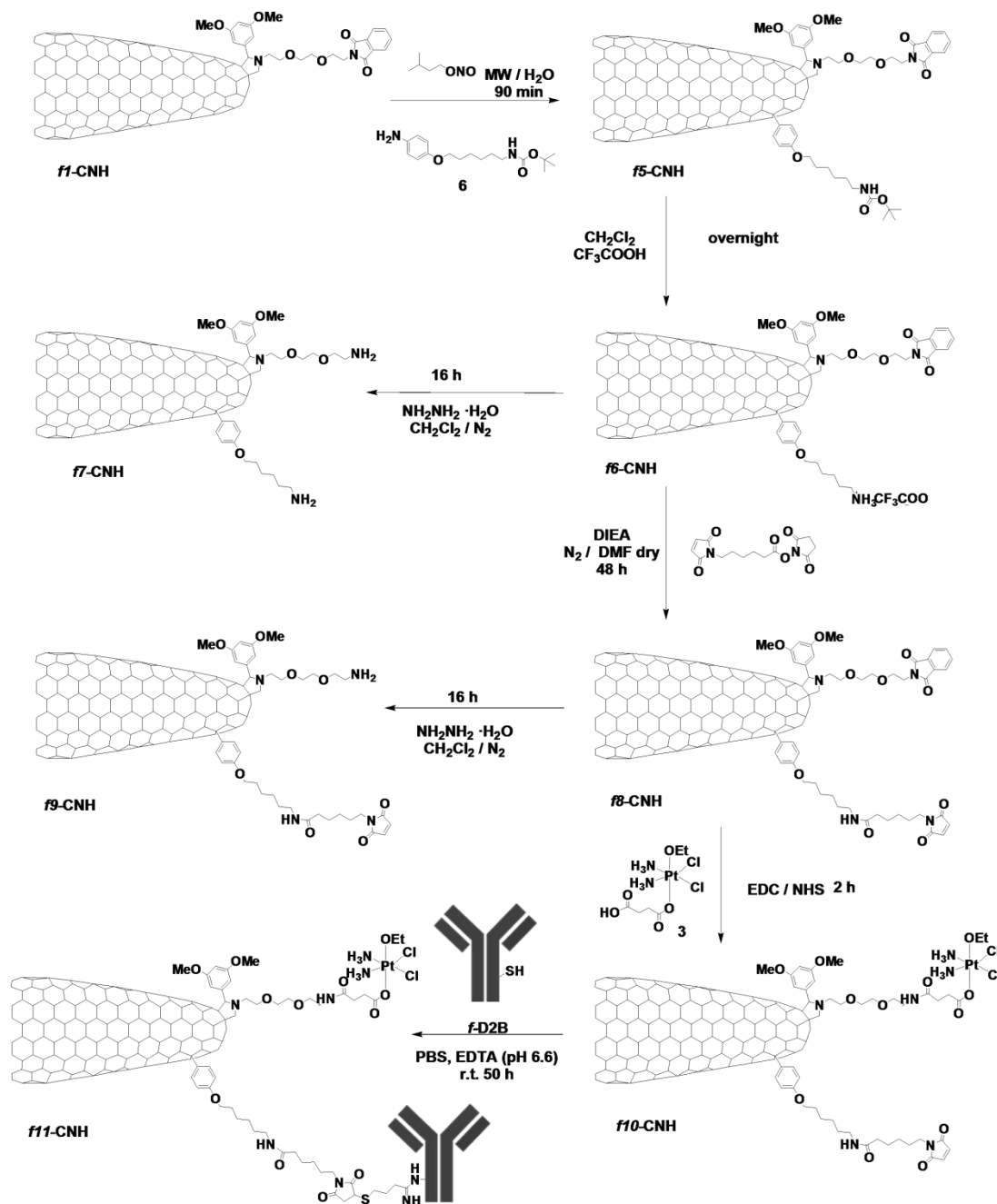
Afterwards, a selective deprotection of Boc-protected amines in acid media was carried out yielding the derivative f6-CNH. The Kaiser test yielded 100 μmol of free amines per gram of CNHs and the TGA yielded 319 μmol of functional group per gram of CNHs (Fig. S3, ESI[†]; table 1). The data from the TGA was calculated according to the removed organic material: the difference between the weight loss of the protected derivative and the deprotected one. The posterior deprotection of these nanohorns in basic medium turned out f7-CNH with 139 μmol of total free amines per gram of CNHs according to the Kaiser test. The TGA analysis yielded the release of 257 amines (Fig. S3,

ESI⁺; table 1). This derivative f7-CNH has enhanced solubility in comparison with pristine CNHs. The decrease in weight loss observed for the deprotected derivatives f6-CNH and f7-CNH (blue and red lines in Fig. S4, ESI⁺) agrees with the removing of organic material in every deprotection step.

Continuing with the preparation of the CNHs derivatives, 6-maleimidohexanoic acid NHS ester was added to f6-CNH to get the focal point for the posterior union of the Ab in f8-CNH. Then, phthalimide was selectively eliminated from f8-CNH by reaction in basic medium, yielding the necessary intermediate f9-CNH to attach the prodrug 3. The TGA and Kaiser Test results of f8-CNH

and f9-CNH are summarized in table 1. In this case, TGA and Kaiser Test data agree probably as a consequence of the increased solubility of these materials.

Prodrug 3 was finally attached to f9-CNH yielding the derivative f10-CNH. This reaction was carried out in absence of light in order to avoid undesirable reactions of the prodrug. Derivatives f9-CNH and f10-CNH were analysed by TGA under air (Fig. S4, ESI⁺). With this method the amount of metal in the sample can be detected after a complete oxidation. The introduction of 44 μmols of drug per gram of CNHs in f10-CNH was calculated from the TGA (table 2).



Scheme 2 Synthesis of functionalised carbon nanohorns f7-CNH, f10-CNH and f11-CNH.

Table 2 Amounts of Ab or cisplatin per gram of CNHs.

Sample	μmol antibody / g. CNHs	μmol cisplatin / g. CNHs
f4-CNH	1.06	n/a ^[a]
f7-CNH	n/a ^[a]	n/a ^[a]
f10-CNH	n/a ^[a]	44
f11-CNH	1.47	44

[a] n/a indicates there is no drug or Ab in the hybrid.

Further proof of the incorporation of the platinum compound in the nanohorns was achieved by the analysis of the derivative f10-CNH using X-ray photoelectron spectroscopy (XPS). This is a semi-quantitative technique that provides information about the elemental composition of the sample as well as about the existent type of bonds.⁶⁰ The Pt 4f spectrum of f10-CNH satisfactorily fitted with two doublets in which the most intense peak of everyone (Pt 4f_{7/2}) appeared at 73.3 and 74.7 eV, demonstrating the presence of platinum in the sample. An energy of 73.5 eV has been previously assigned to the Pt 4f_{7/2} component of Pt 4f in pure PtCl₂ in which Pt is in Pt (II) form and energies between 74.6 and 75 eV have been assigned to PtO₂ and H₂PtCl₆ compounds in which Pt is in its Pt(IV) form.⁶⁰ On the other hand, the presence of peaks associated to Pt (II) compounds in the spectra of Pt(IV) compounds was also expected as it has been previously reported that the exposure of Pt (IV) complexes to X-ray radiation using MgK α irradiation (the one uses in our experiment) causes a reduction of Pt (IV) into Pt (II).⁶¹

In the last stage, the thiolated Ab previously synthesized was attached to the maleimido groups by reaction in PBS-EDTA (4 μM) during 60 h yielding the derivative f11-CNH. The pH of the reaction medium was 6.6 as in the previous synthesis of f4-CNH. In the same way, the success of the addition was demonstrated by the absence of free thiol groups in the crude of reaction by Ellman's test. After cleaning by filtration, f11-CNH was analysed by thermogravimetric analysis in N₂, observing a weight loss of 44% at 600 °C under N₂, corresponding to 1.47 μmol of Ab per gram of CNHs (Fig. S5, ESI[†]; table 2).

Furthermore, f11-CNH derivative was also analysed by XPS. The Pt 4f_{7/2} spectrum of this sample also fitted with two doublets at 73.3 and 74.7 eV according to the presence of the platinum prodrug. Interestingly, a peak at 164.3 eV in the spectrum indicated the presence of S 2p nuclei in the sample, which are due to the presence of the Ab (Fig. S6, ESI[†]).

All the synthesized derivatives were analysed by transmission electron microscopy (TEM) to complete the characterization. No changes were observed in the spherical morphology of CNHs after functionalization. In addition, an improvement in the dispersion with increasing the degree of functionalization was perceived (Fig. 1).

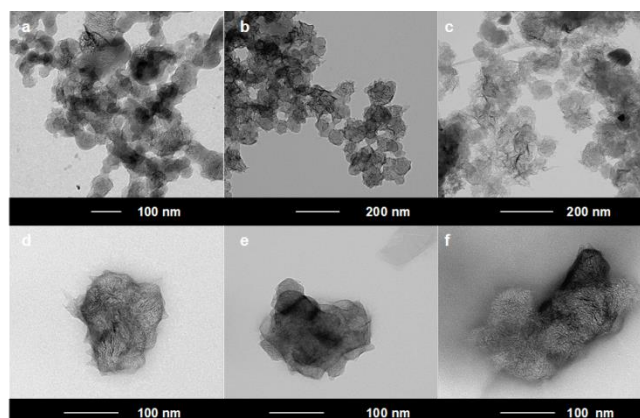


Fig. 1 TEM images of p-CNH (a), f4-CNH (b), f7-CNH (c), f10-CNH (d) and f11-CNH in H₂O solution (e) and PBS solution (f).

As an overview, the presence of cisplatin and Ab in the biologically significant compounds is summarized in table 2.

Interaction with cells

As previously highlighted, the main objective of this work was to selectively target drugs towards cancer cells. So to investigate whether our hybrids were able to get this goal, the biological properties of the complexes f4-CNH, f7-CNH, f10-CNH and f11-CNH were analysed. In this way, different techniques were carried out in order to check the binding specificity, the uptake and the cytotoxicity of these different nanosystems. Moreover the presence of D2B Ab on the surface of the different hybrids was analysed to confirm their correct functionalization.

Flow cytometry to investigate the presence of D2B antibody on the CNH surface. Flow cytometry was applied to analyse the interaction between cells and nanostructures (i.e. binding and uptake) and also to check if the Abs are linked to the CNH surface. Therefore, to demonstrate that the Abs are bound to the nanosystems, we applied a goat-anti-mouse Ab FITC labelled (Gam-FITC) which is able to recognize the murine D2B Ab. As negative control we analysed f7-CNH not conjugated with D2B Ab. The FITC fluorescence signal observed on f11-CNH, Fig. 2 b (mean fluorescence intensity, MFI value = 33), demonstrated the presence of Abs on the CNH surface. The very low autofluorescence and scattering signals of f11-CNH alone were depicted in Fig. 2 a (MFI value = 65). Moreover, a modest signal was observed with the negative control f7-CNH stained with Gam-FITC reagent (Fig. 2 c, MFI value = 476), probably due to a limited non-specific absorption of the staining Ab-FITC on the nanosystem surface. Positive signals, similar to those observed with f11-CNH, were obtained analysing f4-CNH hybrid (i.e. drug unloaded and Ab conjugated), demonstrating the presence of Abs on the CNH surface (data not shown).

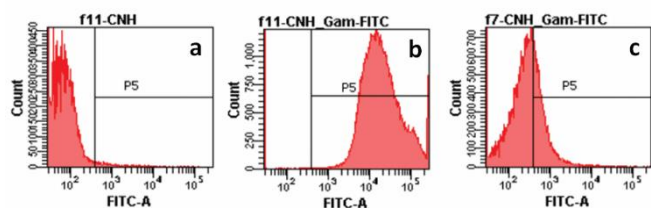


Fig. 2 Flow cytometry analysis of: a) f11-CNH alone, b) f11-CNH stained with Gam-FITC reagent, c) f7-CNH (no Ab conjugated, negative control) stained with Gam-FITC reagent.

Raman spectroscopy. The strong intensity of the Raman signal from carbon nanostructures is a useful tool to identify them in cells⁷ and tissues.^{5,6} Moreover, Raman technique has the advantages of being a non-destructive technique and it does not need external contrast-enhancing agents. Taking this into account, the ability of CNH hybrids to interact with different cancerous cells was analysed by Raman spectroscopy.

CNHs can be identified by Raman spectroscopy due to the presence of two characteristic bands at around 1,600 (G-band) and 1,320 (D-band) cm^{-1} , related, respectively, to the sp^2 π -conjugated carbons and to the sp^3 non conjugated carbons considered to be defects of the CNH structure; furthermore their strong absorption/scattering makes it possible to identify them also with optical images in which dark spots can be observed where they accumulate. Raman spectra were registered at single-cell level after 3 h of CNH incubation with cells. Firstly, the spectra of PC-3-PSMA cells alone were recorded and they clearly do not show the typical CNH Raman signature (Fig. 3 b, cell 2 and 3); the spectra of the glass slide was also recorded (i.e. background signal, Fig. 3 b, point 1). In Fig. 3 c-d, active targeting of PC-3-PSMA cells using f4-CNH (concentration of $62.5 \mu\text{g mL}^{-1}$) was observed. The images, observed with the optical microscope (20x magnification) of the μ -Raman instrument, allow to see dark spots in many cells (Fig. 3 c). The Raman spectrum collected on these cells clearly identifies the characteristic spectrum of the CNH (Fig. 3 d). Conversely, the cell image of Fig. 3 c shows that in A431 cells dark spots are almost absent. Correspondingly, a low intensity CNH spectrum can be observed only for the few cells for which some spots are observed (Fig. 3 f). This shows that specific interactions are almost absent in A431 (PSMA⁻) cells treated with f4-CNH at the same concentration ($62.5 \mu\text{g mL}^{-1}$).

Once the ability of f4-CNH (i.e. D2B-CNHs) to selectively bind PSMA⁺ cancer cells was demonstrated, the next step was to analyse the binding capability of f11-CNH (i.e. CNHs conjugated to Ab and drug). A high f11-CNH accumulation was observed in PC-3-PSMA cells by the optical microscope (black spots in Fig. S7, ESI[†]). Moreover, Raman spectroscopy spectra collected at single-cell level from randomly selected cells showed the characteristic Raman signature of CNHs (Fig. S7, ESI[†]) demonstrating the presence of the nanostructures and, therefore, the uptake into these Ag⁺ cells. The main paragraph text follows directly on here.

Binding analysis of the different hybrids on PSMA⁺ cells by flow cytometry. In a subsequent series of experiment, the

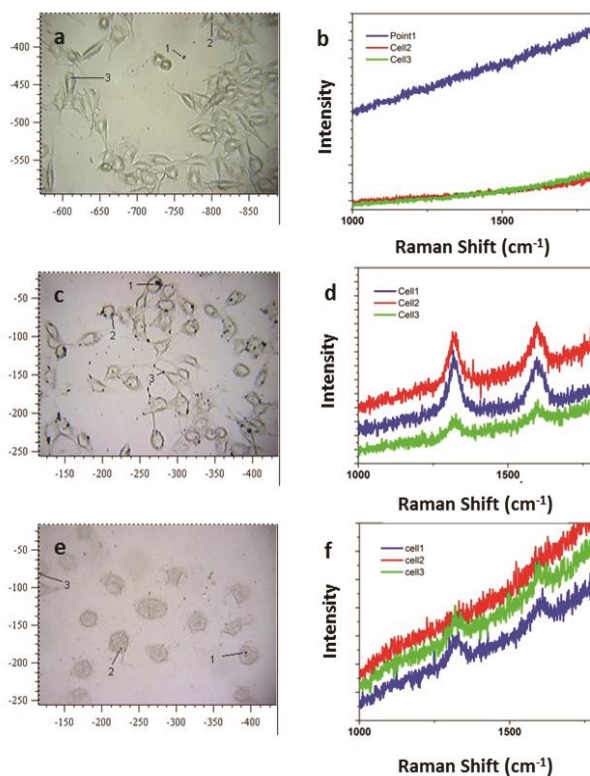


Fig. 3 Bright-field microscopy images and Raman spectra collected at 633 nm of PC-3-PSMA cells alone (a-b), PC-3-PSMA cells incubated with f4-CNH at $62.5 \mu\text{g mL}^{-1}$ (c-d) and A431 cells, PSMA⁻, incubated with f4-CNH at $62.5 \mu\text{g mL}^{-1}$ (e-f).

binding and specificity of f11-CNH (D2B-CNHs) were analysed by flow cytometry on both PC-3-PSMA and PC-3 wild type (WT, PSMA⁻) cells at different CNH concentrations (Table 3). In these assays we used Gam-FITC reagent to show the binding (i.e. at 4°C) of CNHs on PSMA⁺ cells. With this protocol we detected the binding of the derivatives to the cells staining the D2B Ab linked to the CNH surface.

Table 3 Binding at 4°C of f11-CNH serial dilution on PSMA⁺ cells. MFI values obtained by flow cytometry were normalized (MFI sample/MFI Gam-FITC) with the control.

CNHs $\mu\text{g mL}^{-1}$	PC-3-PSMA cells	PC-3 WT (PSMA ⁻) cells
	f11-CNH	f11-CNH
62.5	8.8 ± 1.0	0.9 ± 0.1
125	14.0 ± 1.0	0.8 ± 0.5
250	17.7 ± 0.7	0.7 ± 0.5

As expected, f11-CNH derivative showed on the PSMA⁺ cells a gain of the signal with respect to the control signals when increasing CNH concentration were assessed; conversely, any increment of the signal with respect to the control was observed when increasing concentrations of f11-CNH were incubated with PSMA⁻ cells (i.e. PC-3 WT cells, Table 3). Moreover, a CNH sample was also washed by centrifugation to change the buffer to be sure that the positive signals detected when f11-CNH derivative was incubated with PSMA⁺ cells were not due to the presence of traces of free Ab in the batch. When a pre-centrifuged f11-CNH dispersion at $250 \mu\text{g mL}^{-1}$ was incubated with PC-3-PSMA cells the normalized MFI value was

quite superimposable to the value obtained using the same f11-CN H dispersion not washed by centrifugation. (i.e. 17.2 versus 17.7 for the washed and unwashed f11-CN H, respectively). Thus the fluorescent signal detected by flow cytometry is absolutely due to the binding of f11-CN H on the cell surface.

Afterward, a saturation experiment was carried out at +4°C to better investigate the binding capability of f11-CN H on PC-3-PSMA cells (Fig. 4). The PSMA Ag saturation was reached at a f11-CN H concentration of about 200 $\mu\text{g mL}^{-1}$ (i.e. D2B-CN H); this saturation curve allowed us to confirm the specific binding of f11-CN H to the PSMA⁺ cells.

Additionally, a competition binding assay was performed to strongly confirm the binding specificity of f11-CN H hybrids on PSMA⁺ cells. We analysed the binding signals of a fixed concentration of biotinylated D2B Ab to PC-3-PSMA cells in presence of f11-CN H serial dilution. The decreasing of the fluorescence signal associated to the cells stained with streptavidin-RPE-D2B-biotin complex versus the CN H concentrations is shown in Fig. S8, ESI⁺; we can appreciate that when the concentration of the f11-CN H hybrid is increased, a reduction of D2B-biotin staining is observed. So it is demonstrated a competition between f11-CN H hybrid and free biotinylated Ab, D2B-biotin, for PSMA sites located on cell surface and consequently the PSMA specificity of our targeted f11-CN H hybrid.

Uptake analysis of the different hybrids into PSMA[±] cells by flow cytometry. The binding to Ag⁺ cells is not enough to increase the targeted/drug-loaded CN H killing specificity and their cytotoxicity; therefore their entrance into the cells is mandatory. In fact, overcoming the cellular membrane is actually one of the main tasks of the CN Hs in the complexes. In order to show that the uptake of f11-CN H into cells was achieved and not only the binding to the cell surface, new flow cytometry analyses were carried out on permeabilized and intact cells. Therefore we compared fluorescence signals of permeabilized and not permeabilized cells after incubation with two different f11-CN H concentrations and staining with Gam-FITC reagent. As summarized in table 4, the normalized MFI value on permeabilized cells are remarkably higher (i.e. signal

from bound and internalised CN Hs) than the signal on non-permeabilized ones (i.e. signal from only bound CN Hs) at each analysed f11-CN H concentration. Therefore, a significant number of CN Hs did not only bind to the cell surface but were also internalised into the cells.

In order to confirm this observation, the same experiment was performed on a second PSMA⁺ cell line, LNCaP cells, and obtained data agree with that measured on PC-3-PSMA cells (table S1, ESI⁺). Moreover the experiment was replicated on PC-3 WT cells, PSMA⁻ cells, where no binding and no internalisation were observed (table S2, ESI⁺).

Table 4 Evaluation of binding and uptake of f11-CN H on PC-3-PSMA cells after incubation for 1 h 30 min at 37°C. MFI values obtained by flow cytometry were normalized (MFI sample/MFI Gam-FITC) with the control.

f11-CN H $\mu\text{g mL}^{-1}$	Binding	Uptake
125	11.2±1.6	20.9±0.1
250	17.5±1.6	41.8±1.0

In vitro evaluation of the cytotoxic effects. The main goal of f11-CN H derivative is to selectively kill PSMA⁺ cancer cells. In order to assess this property, the in vitro cytotoxicity of different CN H derivatives (f10-CN H and f11-CN H) was evaluated on PSMA⁺ cells.

As summarized in table 5, when PC-3-PSMA cells were treated with 2.2 μM in cisplatin of the CN H derivatives, we observed a quite similar toxicity (see a percentage of cell viability around 0.1-0.5%); conversely when we increased the stealth properties of the CN H derivatives by preadsorption step with BSA (i.e. bovine serum albumin) the percentage of cell viability of f10-CN H increased to 66.72 ± 1.78% and the same data remained below 20% for f11-CN H. In the same condition (plus and minus BSA preadsorption), when cells were treated with 2.2 μM of cisplatin alone, the percentage of cell viability was about 95%.

Table 5 Cytotoxicity data of f10-CN H and f11-CN H on PC-3-PSMA, PSMA⁺ cells.

Sample	PC-3-PSMA (PSMA ⁺)	
	Minus BSA	Plus BSA
f10-CN H	0.46 ± 0.31%	66.72 ± 1.78%
f11-CN H	0.1 ± 0.22%	19.31 ± 0.80%

The non-specific toxicity caused by f10-CN H is clearly due to an uncompleted masking of the CN H surface; in fact when the stealth properties were increased by protein absorption, the specificity of the f11-CN H was improved with respect to the f10-CN H derivative. Additionally, when PC-3 WT cells, PSMA⁻, were treated with f11-CN H (i.e. cisplatin concentration 1.1 μM) without BSA pre-coating, the percentage of viable cells was 77.60 ± 6.66%, whereas the cell viability of PSMA⁺ cells dropped to 28.31 ± 3.55% when incubated with the same derivative concentration.

According to these results, our target hybrid f11-CN H is able to more selectively kill PSMA⁺ cancer cells in contrast to the

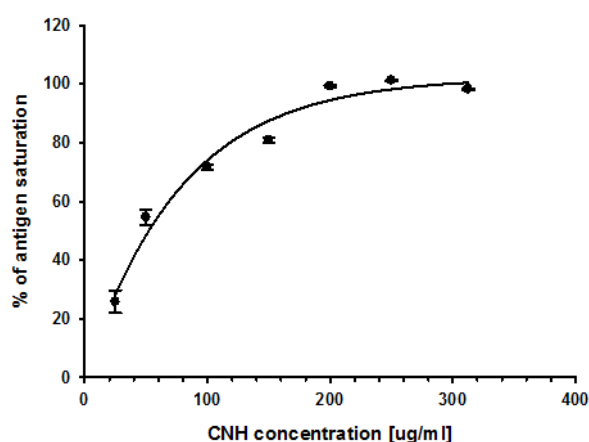


Fig. 4 Saturation binding curve of f11-CN H at 4°C on PC-3-PSMA cells.

cisplatin-functionalised carbon nanohorns without antibody (i.e. f10-CNH). Moreover it is also important to highlight that the killing efficacy of same dose of cisplatin was dramatically increased when carried to the tumour cells by the Ab-CNHs. The cytotoxicity data, obtained when a BSA pre-incubation was performed, suggest that increased CNH stealth properties by coating with PEG chains (i.e. pegylation),^[62] with disordered polypeptide chains comprising the small residues Pro, Ala and Ser (i.e. PASylation),^[63] or with biomimetic leukocyte membranes,^[64] could lead a nanosystem with improved selectivity.

Experimental Section

Synthesis and characterization of carbon nanohorns derivatives

Techniques. Microwave irradiations were carried out in a CEM Discover reactor, with infrared pyrometer, pressure control system, stirring and air-cooling option. UV-vis-NIR experiments were carried out on a Varian Cary 5000 spectrophotometer. The thermogravimetric analyses (TGA) were performed with a TGA Q50 (TA Instruments) at 10 °C min⁻¹ under N₂. For the transmission electron microscopy (TEM) several drops of CNHs solutions in MeOH (2.5·10⁻² mg mL⁻¹) were placed on a copper grid (3.00 mm, 200 mesh, coated with carbon film). After being dried under high vacuum overnight, the sample was investigated by TEM using a Philips EM 208 with an accelerating voltage of 100 kV. Photoelectron spectra (XPS) were obtained with a VG Escalab 200R spectrometer equipped with a hemispherical electron analyser with a pass energy of 50 eV and a Mg K α (h ν = 1,254.6 eV) X-ray source, powered at 120 W. Binding energies were calibrated relative to the C 1s peak at 284.8 eV. High-resolution spectra envelopes were obtained by curve fitting synthetic peak components using the software "XPS peak." Symmetric Gaussian-Lorentzian curves were used to approximate the line shapes of the fitting components. Atomic ratios were computed from experimental intensity ratios and normalized by atomic sensitivity factors. ¹H-NMR and ¹³C-NMR spectra were recorded in solvent on a Varian Inova 400 spectrometer operating at 399.78 MHz for ¹H and 100.53 for ¹³C. The value of chemical shift (δ) are quoted in parts per million (ppm) and the coupling constants (J) in Hertz (Hz).

Materials. Solvents were purchased from SDS and Fluka. Chemicals were purchased from Sigma-Aldrich and used as received without further purification. CNHs were purchased from Carbonium s.r.l. (Padova, Italy) and used without purification. Amino acid 4 and aniline derivative 6 were synthesized following the literature procedure.⁵⁰⁻⁵³

Synthesis of c,c,t-[Pt(NH₃)₂Cl₂(OH)(OEt)], 2: In absence of light, cis-[Pt(NH₃)₂Cl₂] (0.20 g, 0.67 mmol) was suspended in absolute EtOH (250 mL) and heated to 70 °C. A solution of H₂O₂ (0.5 mL, 50%) was added to this suspension with vigorous stirring. After 5 h at elevated temperature the solid dissolved to afford a

bright yellow solution. After cooling at room temperature, the solution volume was reduced to near dryness on a rotary evaporator and Et₂O (50 mL) was added to precipitate the product as a light yellow solid. The solid was collected and washed with ice cold EtOH and Et₂O. Yield was 98% (0.236 g, 0.65 mmol). ¹H-NMR (500 MHz, [D₆]-DMF, 25 °C): δ = 10.44 (s, 1H, OH); 6.018 (s, br, 6 H, NH₃); 3.58 (q, 2 H, CH₂); 1.10 ppm (q, 3 H, CH₃). m.p. 172–175 °C.

Synthesis of c,c,t-[Pt(NH₃)₂Cl₂(OEt)(O₂CCH₂CH₂CO₂H)], 3: Compound 2 (5·10⁻² g, 0.14 mmol) was dissolved in 2 mL of dry DMF. Succinic anhydride (2.1·10⁻² g, 0.21 mmol) in dry DMF (1 mL) was added to this solution and the solution was stirred for 4 h at 75 °C under N₂. The resulting solution was dried in vacuum to leave dark yellow oil, which was dissolved in a small amount of acetone. Addition of Et₂O precipitated a solid that was collected and dried in vacuum to leave the product as a pale yellow powder in 35% yield (2.3·10⁻² g, 0.05 mmol). ¹H-NMR (500 MHz, [D₆]-DMF, 25 °C): δ = 12.36 (m, 1 H, CO₂H); 6.14 (m, 6 H, NH₃); 3.52 (s, 2 H, CH₂); 2.95 (s, 2 H, CH₂); 2.78 (s, 2H, CH₂); 1.01 ppm (t, 3 H, CH₃). m.p. (decomposition), 120–124 °C.

Modification of the antibody (f-D2B): 1.17 mg of EDTA were added to a D2B solution (1 mL, 1.5 mg mL⁻¹) in PBS to afford 4mM and NaHCO₃ saturated (0.1 mL). A freshly prepared solution of 2-iminothiolane·HCl in water (10 μ L, 2 mg mL⁻¹) was added. The mixture was shaken for 2 h at 30 °C, and then it was incubated over night at 4 °C. Finally, the excess of 2-IT was removed by dialysis (MWCO = 500 - 1,000 Da) against PBS/EDTA 4 mM. The number of free sulfhydryl groups introduced in f-D2B was assessed by Ellman's assay to be approximately 1 per Ab.

Synthesis of f1-CNH. Pristine CNHs (25 mg) were suspended in CH₂Cl₂ (5 mL) with the aldehyde 5 (110 mg, 0.66 mmol) and the amino acid 4 (211 mg, 0.66 mmol) in a microwave quartz vessel; after sonication for 5 min, the solvent was evaporated with a N₂ stream, the vessel was closed and introduced into a monomode microwave where the mixture was irradiated for 45 min at different power and temperature.⁵⁰ After this period of time, the crude was re-suspended in 75 mL of CH₂Cl₂ and sonicated for 5 min. The solution was filtered on a Millipore membrane (PTFE, 0.2 μ m) and the collected black solid was washed by cycles of sonication and filtration using three different mixtures of solvents: (i) 100 mL of MeOH/HCl (37%) in a proportion 3:1, (ii) 75 mL of MeOH and (iii) 75 mL of CH₂Cl₂ (sonicated and filtered) and finally dried under high vacuum affording 24 mg of f1-CNH.

Synthesis of f2-CNH. f1-CNH (30 mg) were suspended in CH₂Cl₂ (30 mL) with hydrazine (9 mL, 0.06 mol) and the mixture was stirred for 16 h at room temperature under N₂. The crude was filtered on a Millipore membrane (PTFE, 0.2 μ m) and washed by cycles of sonication and filtration with CH₂Cl₂ (75 mL) and MeOH (100 mL), and finally dried under high vacuum affording 28 mg of f2-CNH.

Synthesis of f3-CNH. f2-CNH (13 mg, 6.5 μmol of amine groups) were suspended in dry DMF (5 mL) and neutralized with dry DIEA (57 μl , 325 μmol) under N_2 . A solution of 6-Maleimidohexanoic acid N-hydroxysuccinimide ester (40 mg, 130 μmol) in DMF (2 mL) was added. The reaction was sonicated for 20 min and then stirred at r.t. under N_2 for 48 h. The obtained f3-CNH were extensively washed by filtration (on a Millipore membrane (PTFE, 0.2 μm) with DMF, MeOH and Et_2O , and then dried under high vacuum. Yield: 13 mg.

Synthesis of f4-CNH. The maleimido-derived f3-CNH (10 mg) was dispersed in PBS/EDTA (20 mL, 4 mM) and the f-D2B solution (3.6 mL, 2 μM) was added and the mixture was shaken for 60 h at r.t. The obtained f4-CNH was washed by filtration on a Millipore membrane (PTFE, 0.2 μm) with PBS. The resulting Ab-conjugate f4-CNH was stored at 4 $^\circ\text{C}$ as dispersions of 0.5 mg mL^{-1} in PBS (pH 7.4). The solubility is around 0.4 mg mL^{-1} in PBS/EDTA (4 mM).

Synthesis of f5-CNH. f1-CNH (40 mg) were sonicated in deionized water together with Boc-protected aniline 6 (1.53 g, 6.92 mmol) for 10 min in a microwave glass vessel. Finally, isoamyl nitrite (0.44 mL, 3.34 mmol) was added, and a condenser was placed. The mixture was irradiated at 80 $^\circ\text{C}$ with a monomode microwave working at 100W for 30 min, and after addition of a new aliquot of isoamyl nitrite (0.44 mL, 3.34 mmol), at 30W for 60 min. After cooling at room temperature, the crude was filtered on a Millipore membrane (GTTT, 0.2 μm). The collected black solid was washed using cycles of sonication and filtration with MeOH until the filtrate was clear and finally dried under high vacuum affording 36 mg of double functionalised intermediate f5-CNHs.

Synthesis of f6-CNH. The double protected intermediated (f5-CNH, 90 mg) was sonicated in CH_2Cl_2 (100 mL) for 5 min. Then, trifluoroacetic acid (100 mL) was added. The mixture was stirred for 48 h at room temperature. The crude was filtered on Millipore membrane (PTFE, 0.2 μm) and washed by cycles of sonication and filtration with CH_2Cl_2 (75 mL) and Et_2O (50 mL), and finally dried under high vacuum affording 80 mg of f6-CNH.

Synthesis of f7-CNH. f6-CNH (12 mg) were suspended in CH_2Cl_2 (12 mL) with hydrazine (3.6 mL, 0.024 mol) and the mixture was stirred for 16 h at room temperature. The crude was filtered on a Millipore membrane (PTFE, 0.2 μm) and washed by cycles of sonication and filtration with CH_2Cl_2 (75 mL) and MeOH (100 mL) and Et_2O (50 mL), and finally dried under high vacuum affording 10.5 mg of f7-CNH.

Synthesis of f8-CNH. f6-CNH (60 mg, 13.75 μmol of amine groups) were suspended in dry DMF (5 mL) and neutralized with dry DIEA (200 μl , 1140.35 μmol) under N_2 . A solution of 6-Maleimidohexanoic acid NHS ester (85 mg, 276.25 μmol) in DMF (4 mL) was added. The reaction was sonicated for 10 min and then stirred at room temperature under N_2 for 48 h. The obtained f8-CNH was extensively washed by filtration on a

Millipore membrane (PTFE, 0.2 μm) with DMF, MeOH and Et_2O , and then dried under high vacuum affording 56 mg.

Synthesis of f9-CNH. f8-CNH (52 mg) were suspended in CH_2Cl_2 (52 mL) with hydrazine (15.6 mL, 0.1 mol) and the mixture was stirred for 16 h at room temperature. The crude was filtered on a Millipore membrane (PTFE, 0.2 μm) and washed by cycles of sonication and filtration with CH_2Cl_2 (75 mL) and MeOH (100 mL) and Et_2O (50 mL), and finally dried under high vacuum affording 45 mg of f9-CNH.

Synthesis of f10-CNH. In absence of light, an aqueous solution of N-hydroxysuccinimide (NHS) (20 mL, 1.0 mM) was added to an equal volume of an aqueous 1.0 mM solution of 1-ethyl-3-[3-dimethylaminopropyl]carbodiimide hydrochloride (EDC) and the resulting solution was allowed to stand at room temperature for 10 min. c,c,t-[Pt(NH₃)₂Cl₂(OEt)(O₂CCH₂CH₂CO₂H)] 3 (7 mg) in MQ water was added to this solution. After 10 min, f9-CNH (42 mg) were added. The solution was sonicated for 3 min, heated to 50 $^\circ\text{C}$ for 2 h and then agitated overnight at room temperature. The crude was filtered on a Millipore membrane (GTTT, 0.2 μm) and washed with MQ water. 40 mg of f10-CNH were obtained.

Synthesis of f11-CNH. The maleimido-derived f10-CNH (18 mg) was dispersed in PBS/EDTA (20 mL, 4 mM) and a f-D2B solution (17 mL, 6.7 μM) was added. The mixture was shaken for 60 h at room temperature until there was no Ab was detected in the supernatant by UV-Vis-NIR spectroscopy. Finally, the resulting f11-CNH was washed by filtration on a Millipore membrane (PTFE, 0.2 μm) with PBS. The resulting Ab-conjugate f11-CNH was stored at 4 $^\circ\text{C}$ as dispersions of 0.25 mg mL^{-1} in PBS/EDTA (pH 7.8).

Interaction with cells

Raman spectroscopy. Different cell line, PC-3-PSMA PCa cells (i.e. transfected to express the PSMA antigen) and A431 cells (PSMA⁻) were incubated with 62.5 $\mu\text{g mL}^{-1}$ of f4-CNH at 37 $^\circ\text{C}$ for 3 h and then, after washing and fixating with 2% paraformaldehyde, Raman spectra were registered at single-cell level with a 20x objective and a controlled XY stage using a Renishaw inVia confocal μ -Raman instrument equipped with a He-Ne laser. Power lower than 1 mW at 633 nm was used for excitation.

Cell lines and anti-PSMA antibody. PC-3 WT (human prostate tumour cells, PSMA⁻), LNCaP (human prostate tumour cells, PSMA⁺) and A431 (human epidermoid carcinoma cells, PSMA⁻) were obtained from American Type Culture Collection (ATCC, Manassas, VA, Rockville, USA). PC-3-PSMA cells (i.e. also called PC-3-PIP) stably transfected to express human PSMA, were kindly provided by Dr. Warren Heston (Department of Cancer Biology, Cleveland Clinic Main Campus).²³ PC-3, PC-3-PSMA and LNCaP cells were cultured in RPMI 1640 Medium supplemented with 2 mM L-Glutamine and 0.01 M HEPES and maintained at 37 $^\circ\text{C}$ in a humidified atmosphere containing 5% CO₂ and 90% of

humidity. A431 cells were cultured in DMEM medium added with the same reagents and also with 1 mM Na pyruvate. Moreover all the media were supplemented with 10% heat-inactivated foetal bovine serum (FBS) (Invitrogen, New York, NY, USA) and antibiotics (0.1 mg mL⁻¹ streptomycin and 100 units mL⁻¹ penicillin G (Sigma-Aldrich, St Louis, MO, USA).

The anti-PSMA mouse antibody D2B was purified from the hybridoma supernatant by affinity chromatography on Protein G Sepharose 4 Fast Flow (GE Healthcare Europe GmbH, Milano, Italy).

Detection of the D2B-Ab on the CNH surface by flow cytometry. We applied flow cytometry to confirm the presence on the Ab on CNH surface; briefly f11-CNH, f4-CNH and f7-CNH were incubated with a goat anti-mouse (Gam) antibody, FITC-labelled (BD Biosciences, Milan, Italy), for 1 h at 4 °C in PBS plus BSA 0.2%. Then CNHs were washed with cold PBS and the bound fluorescence was analysed with a BD FACSCanto II apparatus (BD Biosciences).

Analysis of the CNH interaction with cells by flow cytometry

Binding. In these assays to show the binding (i.e. at 4°C) of the CNHs on PSMA^{+/−} cells we used Gam-FITC reagent; negative cells were applied to confirm also the target specificity. With this protocol we recognised the derivatives bound to the cells staining the D2B Ab linked to the CNH surface. To be sure that the positive signals observed in the flow cytometry analysis were not due to the presence of free D2B antibody in the f11-CNH batch, we also analysed a sample that was centrifuged before the analysis to change the buffer and eliminate free D2B antibody, if present. Briefly, 200,000 cells were incubated at 4°C for 1 h with three different concentrations of f11-CNH (i.e. 62.5, 125 and 250 µg mL⁻¹) and then, after two washing steps, stained with Gam-FITC reagent. Finally, CNHs were washed with cold PBS and the fluorescence associated with cells was analysed with the flow cytometer. The same protocol was applied to create the saturation binding curve of f11-CNH to PC-3-PSMA cells where dilutions ranging from 25 to 500 µg mL⁻¹ were used.

Competition-binding. In the competition-binding experiment the same number of cells was co-incubated with different derivative concentrations, ranging from 0 µg mL⁻¹ to 375 µg mL⁻¹, and 1 µg of D2B-biotin Ab for 1h at 4°C, then samples were washed twice with cold PBS buffer and incubated with streptavidin-RPE (Streptavidin labelled with R-Phycoerythrin) for 30 min at 4°C. After a washing step the samples were analysed with the flow cytometer.

Uptake vs Binding. Cells were plated on a 24 well/plate. Then, cells were incubated the day after with two concentrations of f11-CNHs for 1h 30 min at 37°C. They were washed with PBS buffer and detached with PBS-EDTA. For each experimental point a portion of the total cells was permeabilized with 70% MeOH for 1h in ice and then incubated with Gam-FITC for FACS analysis. The residual cells, no permeabilized, were also

incubated with Gam-FITC; at the end of the incubation cells were washed with cold PBS and analysed with a flow cytometer. The binding signal is given by CNHs bound to PSMA antigen on the no permeabilized cells (i.e. surface signal alone); conversely. The uptake data was obtained from the permeabilized cells where we have the addition of both signals due to the CNHs internalised and the CNHs bound to cell surface.

Viability assay. For the viability assays cells were seeded, one day before the assay, at an appropriate cell density in 90 µl of complete medium in 96 well culture microplates; the day after, the cells were incubated in triplicate with 10 µl of serial dilution of f11-CNHs, f10-CNHs or Cisplatin alone at 37°C for 22 h. Then, the cells were washed and incubated for 2 h in the medium supplemented with XTT reagent (Sigma-Aldrich), according to the supplier instructions; finally cell viability was measured at 450 nm with a microplate reader. The percent of cell viability was estimated analysing the values obtained from treated cells with respect to mock treated ones.

Conclusions

A new series of hybrid materials composed of carbon nanohorns as delivery vehicles (Ab-CNH, Drug-CNH, Ab-Drug-CNH and Double Functionalised-CNH) have been synthesized and fully characterized. In particular, cisplatin in a prodrug form and a specific D2B antibody for PSMA⁺ prostate cancer cells have been attached. Different biological experiments have demonstrated the selective binding and uptake of the conjugates with antibody (Ab-CNH and Ab-Drug-CNH) on PSMA⁺ prostate cancer cells. Finally, the selectivity of the derivative Ab-Drug-CNH on PSMA⁺ prostate cancer cells has made possible their selective killing versus PSMA[−] prostate cancer cells. This property is enhanced when the nanosystems are shielded with BSA. In conclusion, we have demonstrated the better ability of f11-CNH to selectively kill PSMA⁺ cancer cells in comparison with the other synthesized CNHs hybrids. Furthermore, this new system offers great potentiality due to the possibility of modifying the type and degree of functionalization. This allows the variation of the quantity of drug or antibody attached to the nanostructure in order to play with the killing efficacy. Similarly, the method is useful to attach different drugs or antibodies opening the way to the treatment of other diseases.

Conflicts of interest

There are no conflicts to declare.

Acknowledgements

G.F. gratefully acknowledges Fondazione Cariverona, Verona Nanomedicine Initiative and Italian Minister of Health RF-2010-2305526 for supporting this work. M.M. thanks the University of Padova (P-DiSC #04BIRD2016-UNIPD). This work was also supported by the Spanish Ministry of Economy and

Competitiveness MINECO (projects CTQ2014-53600-R and CTQ2016-76721-R), by the EU Graphene-based disruptive technologies, Flagship project (no. 696656). M.P., as the recipient of the AXA Chair, is grateful to the AXA Research Fund for financial support. M.P. was also supported by Diputación Foral de Gipuzkoa program Red (101/16).

Notes and references

- 1 S. Lacotte, A. García, M. Décossas, W. T. Al-Jamal, S. Li, K. Kostarelos, S. Muller, M. Prato, H. Dumortier and A. Bianco, *Adv. Mater.*, 2008, **20**, 2421–2426.
- 2 K. Ajima, M. Yudasaka, T. Murakami, A. Maigne, K. Shiba and S. Iijima, *Mol. Pharm.*, 2005, **2**, 475–480.
- 3 T. Murakami, K. Ajima, J. Miyawaki, M. Yudasaka, S. Iijima and K. Shiba, *Mol. Pharm.*, 2004, **1**, 399–405.
- 4 F. C. Pérez-Martínez, B. Carrión, M. I. Lucío, N. Rubio, M. A. Herrero, E. Vázquez and V. Ceña, *Biomaterials*, 2012, **33**, 8152–8159.
- 5 J. Guerra, M. A. Herrero, B. Carrión, F. C. Pérez-Martínez, M. I. Lucío, N. Rubio, M. Meneghetti, M. Prato, V. Ceña and E. Vázquez, *Carbon*, 2012, **50**, 2832–2844.
- 6 G. J. Weiner, *Nat. Rev. Cancer*, 2015, **15**, 361–370.
- 7 Y. Xiao, X. Gao, O. Taratula, S. Treado, A. Urbas, R. D. Holbrook, R. E. Cavicchi, C. T. Avedisian, S. Mitra, R. Savla, P. D. Wagner, S. Srivastava and H. He, *BMC Cancer*, 2009, **9**, 1–11.
- 8 J. Kim, E. I. Galanzha, E. V. Shashkov, H. Moon and V. P. Zharov, *Nat. Nanotechnol.*, 2013, **4**, 688–694.
- 9 R. Marega, F. De Leo, F. Pineux, J. Sgrignani, A. Magistrato, A. D. Naik, Y. García, L. Flamant, C. Michiels and D. Bonifazi, *Adv. Funct. Mater.*, 2013, **23**, 3173–3184.
- 10 F. Riedel, I. Zaiss, D. Herzog, K. Götte, R. Naim and K. Hörmann, *Anticancer Res.*, 2005, **25**, 2761–2766.
- 11 www.cancer.org/cancer/prostatecancer/detailedguide/prostate-cancer-survival-rates.
- 12 M. Kuroki and N. Shirasu, *Anticancer Res.*, 2014, **34**, 4481–4488.
- 13 G. P. Murphy, T. G. Geene, W. T. Tino, A. L. Boyton and E. H. Holmes, *J. Urol.*, 1998, **160**, 2396–2401.
- 14 S. S. Chang, D. S. O. Keefe, D. J. Bacich, V. E. Reuter, W. D. W. Heston and P. B. Gaudin, *Clin. Cancer Res.*, 1999, **5**, 2674–2681.
- 15 H. Liu, P. Moy, S. Kim, Y. Xia, a Rajasekaran, V. Navarro, B. Knudsen and N. H. Bander, *Cancer Res.*, 1997, **57**, 3629–3634.
- 16 R. G. Lapidus, C. W. Tiffany, J. T. Isaacs and B. S. Slusher, *Prostate*, 2000, **45**, 350–354.
- 17 M. Colombatti, S. Grasso, A. Porzia, G. Fracasso, M. T. Scupoli, S. Cingarlini, O. Poffe, H. Y. Naim, M. Heine, G. Tridente, F. Mainiero and D. Ramarli, *PLoS One*, 2009, **4**, e4608.
- 18 M. E. Perico, S. Grasso, M. Brunelli, G. Martignoni, E. Munari, E. Moiso, G. Fracasso, T. Cestari, H. Y. Naim, V. Bronte, M. Colombatti and D. Ramarli, *Oncotarget*, 2016, **7**, 74189–74202.
- 19 X. Wang, L. Yin, P. Rao, R. Stein, K. M. Harsch, Z. Lee and W. D. W. Heston, *J. Cell. Biochem.*, 2007, **102**, 571–579.
- 20 S. S. Taneja, *Rev. Urol.*, 2004, **6**, 19–28.
- 21 M. Meneghetti, A. Scarsi, L. Litti, G. Marcolongo, V. Amendola, M. Gobbo, M. Di Chio, A. Boscaini, G. Fracasso and M. Colombatti, *Small*, 2012, **8**, 3733–3738.
- 22 J. Tykvart, V. Navrátil, F. Sedláč, E. Corey, M. Colombatti, G. Fracasso, F. Koukolík, C. Bařinka, P. Sácha and J. Konvalinka, *Prostate*, 2014, **74**, 1674–90.
- 23 B. Frigerio, G. Fracasso, E. Luison, S. Cingarlini, M. Mortarino, A. Coliva, E. Seregni, E. Bombardieri, G. Zuccolotto, A. Rosato, M. Colombatti, S. Canevari and M. Figini, *Eur. J. Cancer*, 2013, **49**, 2223–2232.
- 24 S. Lütje, C. M. van Rij, G. M. Franssen, G. Fracasso, W. Helfrich, A. Eek, W. J. Oyen, M. Colombatti and O. C. Boerman, *Contrast Media Mol. Imaging*, 2014, **10**, 28–36.
- 25 A. Juzgado, A. Soldà, A. Ostric, A. Criado, G. Valenti, S. Rapino, G. Conti, G. Fracasso, F. Paolucci and M. Prato, *J. Mater. Chem. B*, 2017, **5**, 6681–6687.
- 26 J. R. Adair, P. W. Howard, J. a Hartley, D. G. Williams and K. a Chester, *Expert Opin. Biol. Ther.*, 2012, **12**, 1191–1206.
- 27 S. Chen and Y. Cao, *JSM Cell*, 2014, **2**, 1006.
- 28 P. D. Senter, *Curr. Opin. Chem. Biol.*, 2009, **13**, 235–44.
- 29 P. J. Carter and P. D. Senter, *Cancer J.*, 2008, **14**, 154–169.
- 30 A. G. Polson, J. Calemine-Fenau, P. Chan, W. Chang, E. Christensen, S. Clark, F. J. de Sauvage, D. Eaton, K. Elkins, J. M. Elliott, G. Frantz, R. N. Fuji, A. Gray, K. Harden, G. S. Ingle, N. M. Kljavin, H. Koeppen, C. Nelson, S. Prabhu, H. Raab, S. Ross, D. S. Slaga, J.-P. Stephan, S. J. Scales, S. D. Spencer, R. Vandlen, B. Wranik, S.-F. Yu, B. Zheng and A. Ebens, *Cancer Res.*, 2009, **69**, 2358–64.
- 31 P. Chames, M. Van Regenmortel, E. Weiss and D. Baty, *Br. J. Pharmacol.*, 2009, **157**, 220–233.
- 32 X. Ma, C. Shu, J. Guo, L. Pang, L. Su, D. Fu and W. Zhong, *J. Nanoparticle Res.*, 2014, **16**, 2497.
- 33 N. Li, Q. Zhao, C. Shu, X. Ma, R. Li, H. Shen and W. Zhong, *Int. J. Pharm.*, 2014, **478**, 644–654.
- 34 C. Tripisciano and E. Borowiak-Palen, *Phys. Status Solidi*, 2008, **245**, 1979–1982.
- 35 C. Tripisciano, K. Kraemer, a Taylor and E. Borowiak-Palen, *Chem. Phys. Lett.*, 2009, **478**, 200–205.
- 36 C. Tripisciano, S. Costa, R. J. Kalenczuk and E. Borowiak-Palen, *Eur. Phys. J. B*, 2010, **75**, 141–146.
- 37 L. Sui, T. Yang, P. Gao, A. Meng, P. Wang, Z. Wu and J. Wang, *Int. J. Pharm.*, 2014, **471**, 157–65.
- 38 J. Li, S. Q. Yap, S. L. Yoong, T. R. Nayak, G. W. Chandra, W. H. Ang, T. Panczyk, S. Ramaprabhu, S. K. Vashist, F.-S. Sheu, A. Tan and G. Pastorin, *Carbon*, 2012, **50**, 1625–1634.
- 39 J. Li, A. Pant, C. F. Chin, W. H. Ang, C. Ménard-Moyon, T. R. Nayak, D. Gibson, S. Ramaprabhu, T. Panczyk, A. Bianco and G. Pastorin, *Nanomedicine*, 2014, **10**, 1465–75.
- 40 S. L. Yoong, B. S. Wong, Q. L. Zhou, C. F. Chin, J. Li, T. Venkatesan, H. K. Ho, V. Yu, W. H. Ang and G. Pastorin, *Biomaterials*, 2014, **35**, 748–59.
- 41 W. Wu, R. Li, X. Bian, Z. Zhu, D. Ding, X. Li, Z. Jia, X. Jiang and Y. Hu, *ACS Nano*, 2009, **3**, 2740–50.
- 42 K. Ajima, A. Maigne, M. Yudasaka and S. Iijima, *J. Phys. Chem. B*, 2006, **110**, 19097–19099.
- 43 K. Ajima, M. Yudasaka, A. Maigne, J. Miyawaki and S. Iijima, *J. Phys. Chem. B*, 2006, **110**, 5773–5778.
- 44 K. Ajima, T. Murakami, Y. Mizoguchi, K. Tsuchida, T. Ichihashi, S. Iijima and M. Yudasaka, *ACS Nano*, 2008, **2**, 2057–2064.
- 45 M. R. DeWitt, A. M. Pekkanen, J. Robertson, C. G. Rylander and M. N. Rylander, *J. Biomech. Eng.*, 2014, **136**, 21003.
- 46 E. R. Jamieson and S. J. Lippard, *Chem. Rev.*, 1999, **99**, 2467–2498.
- 47 M. Groessl, M. Terenghi, A. Casini, L. Elviri and R. Lobinski, *J Anal Spectrom*, 2010, **25**, 305–313.
- 48 M. D. Hall, H. R. Mellor, R. Callaghan and T. W. Hambley, *J. Med. Chem.*, 2007, **50**, 3403–3411.
- 49 S. Dhar, Z. Liu, J. Thomale, H. Dai and S. J. Lippard, *J. Am. Chem. Soc.*, 2008, **130**, 11467–11476.
- 50 N. Rubio, M. A. Herrero, M. Meneghetti, Á. Díaz-Ortiz, M. Schiavon, M. Prato and E. Vázquez, *J. Mater. Chem.*, 2009, **19**, 4407.
- 51 G. Pastorin, W. Wu, S. Wieckowski, J.-P. Briand, K. Kostarelos, M. Prato and A. Bianco, *Chem. Commun.*, 2006, **1**, 1182–4.
- 52 C. C. Forbes, K. M. Divittorio and B. D. Smith, *J. Am. Chem. Soc.*, 2008, **128**, 9211–9218.
- 53 M. Adamczyk, S. R. Akireddy, P. G. Mattingly and R. E. Reddy, *Tetrahedron*, 2003, **59**, 5749–5761.
- 54 R. P. Feazell, N. Nakayama-Ratchford, H. Dai and S. J. Lippard, *J. Am. Chem. Soc.*, 2007, **129**, 8438–8439.

- 55 R. R. Traut, A. Bollen, T. Sun, J. W. B. Hershey, J. Sundberg and L. R. Pierce, *Biochemistry*, 1973, **12**, 3266–3273.
- 56 G. L. Ellman, *Arch. Biochem. Biophys.*, 1959, **82**, 70–77.
- 57 E. Venturelli, C. Fabbro, O. Chaloin, C. Ménard-Moyon, C. R. Smulski, T. Da Ros, K. Kostarelos, M. Prato and A. Bianco, *Small*, 2011, **7**, 2179–2187.
- 58 V. K. Sarin, S. B. H. Kent, J. P. Tam and R. B. Merrifield, *Anal. Biochem.*, 1981, **117**, 147–157.
- 59 R. Singh, L. Kats, W. A. Bla and J. M. Lambert, *Anal. Biochem.*, 1996, **236**, 114–125.
- 60 J. F. Moulder, W. F. Stickle, P. E. Sobol and K. D. Bomben, *Handbook of X-ray Photoelectron Spectroscopy*, Physical Electronics, Inc., Minnesota (United States of America), 1992.
- 61 A. V. Kalinkin, M. Y. Smirnov, A. I. Nizovskii and V. I. Bukhtiyarov, *J. Electron Spectros. Relat. Phenomena*, 2010, **177**, 15–18.